ACS APPLIED MATERIALS & INTERFACES

Research Article

www.acsami.org

Simple Method for Manufacturing Pt Counter Electrodes on Conductive Plastic Substrates for Dye-Sensitized Solar Cells

Yun Gong,[†] Chunhui Li,[†] Xiaoming Huang,[†] Yanhong Luo,[†] Dongmei Li,[†] Qingbo Meng,*[,†] and Bo Brummerstedt Iversen*

[†]Key Laboratory for Renewable Energy, Chinese Academy of Sciences, Beijing Key Laboratory for New Energy Materials and Devices, Beijing National Laboratory for Condensed Matter Physics, Institute of Physics, Chinese Academy of Sciences, Beijing 100190, PR China

[‡]Center for Materials Crystallography, Department of Chemistry and Interdisciplinary Nanoscience Center, Aarhus University, DK-8000 Aarhus, Denmark

ABSTRACT: A novel, facile, and low-cost method was developed for manufacturing Pt counter electrodes (CEs) of dye-sensitized solar cells (DSCs) on the indium tin oxide-coated polyethylene terephthalate (ITO-PET). This press-transferring method reconciled the temperature conflict between the sintering process of thermal decomposition of H_2PtCl_6 and plastic substrates. Cyclic voltammograms, electrochemical impedance spectroscopy, transmittance spectra and photovoltaic performance were characterized to investigate the transferred Pt CEs. It was found that the transferred Pt CEs on ITO-PET exhibited an excellent catalytic activity comparable with traditional electrodes on FTO glasses. On the front-side, an illuminated conversion efficiency of 7.21% was reached with more than 94% efficiency of conventional thermally deposited Pt CEs on FTO glasses, and on the back-side, the illuminated conversion efficiency was 4.86%, which was higher than that for conventional electrodes.

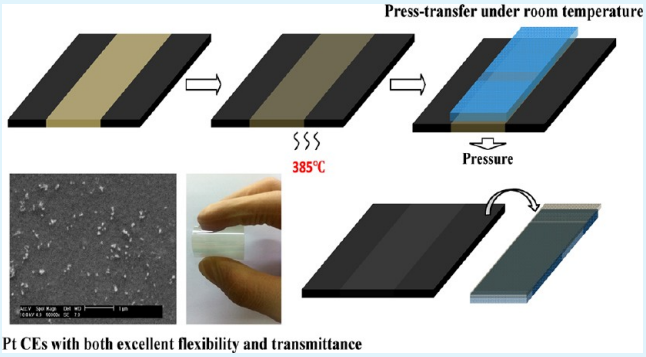

KEYWORDS: *flexible Pt counter electrodes, dye-sensitized solar cell, press-transfer method*

1. INTRODUCTION

Dye-sensitized solar cells (DSCs) have attracted great interests and they are considered as a potential alternative for traditional silicon-based solar cells. The properties of DSCs continue to be improved in past decades and the photoelectric conversion efficiency of DSCs on fluorine-doped tin oxide (FTO) glass substrates now has exceeded 12%.[1,2] Besides being low-cost and environment friendly, DSCs are more convenient in preparing flexible devices than silicon-based solar cells, which is significant for the large-scale commercial application. Recently, flexible DSCs with high efficiency have been reported.[3−5] Stainless steel and Ti sheet were used as flexible substrates and the efficiencies of these cells were more than 7%.[3,5] Photoanodes prepared by the press method on ITO-PEN reached a validated conversion efficiency of 7.6%.[4] To further enhance the performance of flexible DSCs, the flexible counter electrode, one of the most important components, should be optimized to reach a better catalytic ability with triiodide.

Platinum, which shows superior performance in electrocatalytic applications compared with other materials utilized as counter electrodes (CEs) such as metal inorganic compounds,[6−8] conductive polymers,[9−11] and carbon materials,[12−14] has been fabricated on different substrates with many different methods.[15−24] Typically, sputtering is the technique of choice in fabricating Pt CEs and this often results in high efficiencies.[15−17] The properties of sputtered Pt CEs on rigid and flexible substrates have been systematically discussed.[15−17] However, sputtering of Pt CEs leads to an inevitable waste of expensive metal during the fabrication process and the electrode is opaque which makes back-side illumination of the cells impossible. Chemical reduction[18−20] and electrochemical deposition[5,21,22] can be used to prepare transparent Pt CEs on flexible substrates, but the problems with their weak adhesion to the substrates and with the inhomogeneous clusters[23] have not been resolved. Pt CEs prepared by thermal deposition have both good performances in cells and excellent transparency[24] that guarantees the possibility of back-side illumination. However, optimized catalytic performance of thermal deposition of Pt requires a 385 °C thermal treatment, from which most flexible transparent conductive substrates cannot suffer.

In our previous work, we have managed to solve similar temperature conflicts in preparing FTO film on plastic substrates[25] and flexible TiO_2 photoanodes of quantum-dot sensitized solar cells.[26] Here, we present a much simpler method based on press transfer, which preserve the excellent

Received: October 16, 2012
Accepted: January 8, 2013
Published: January 8, 2013

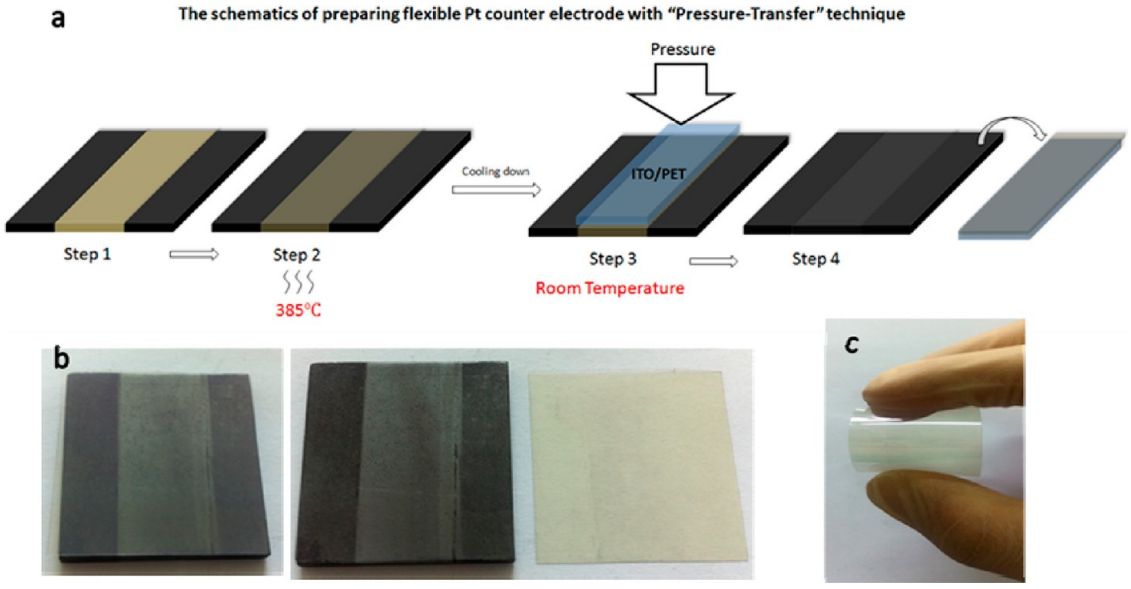

Figure 1. (a) Schematic showing the steps of the new technique for preparation of the flexible transparent Pt counter electrodes. (b) Actual pictures of step 3 and step 4. (c) The final Pt counter electrode with excellent flexibility and transparency.

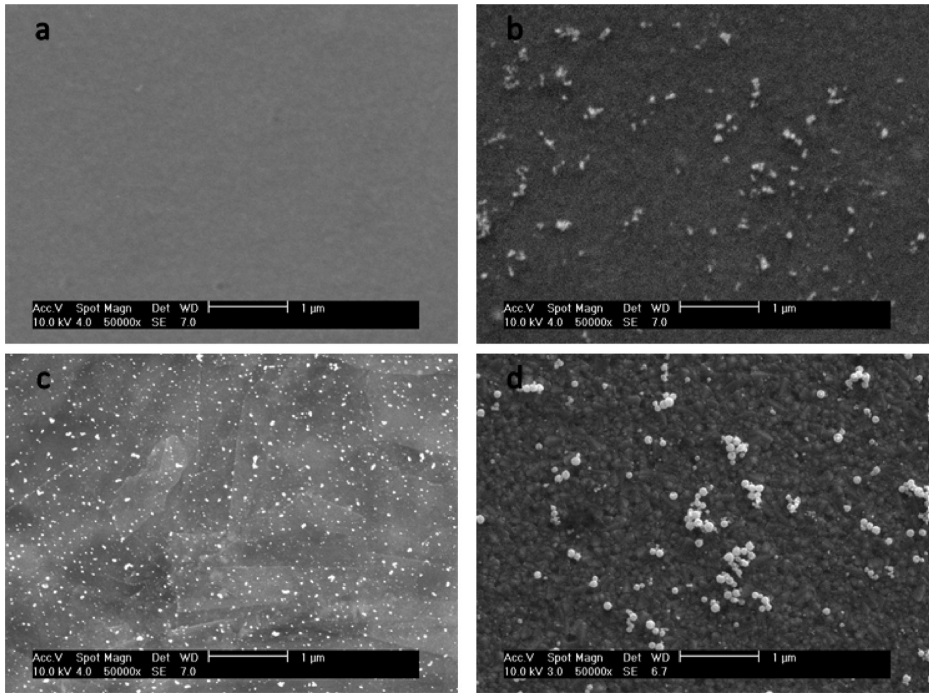

Figure 2. (a) Scanning electron microscopy images of bare ITO-PET substrate, (b) Pt electrodes prepared on ITO-PET by the press transfer method with 100 MPa, (c) Pt electrodes prepared by heating on graphite sheet, and (d) on FTO glass.

properties of Pt from thermal deposition, and we use it to manufacture Pt CEs on indium tin oxide-coated polyethylene terephthalate (ITO-PET) at room temperature. The microstructures, reaction catalytic activity, platinum/electrolyte interface and the optical transmittance of the CEs have been examined. Both front- and back-side illumination photovoltaic performances of DSCs have been investigated with different preparation conditions. The devices prepared with the new method obtained comparable efficiencies with that of the traditional systems.

2. EXPERIMENTAL SECTION

Preparation of Dye-Sensitized TiO_2 Photoanodes. The TiO_2 photoanodes were fabricated on well-cleaned FTO glass (13Ω/□, Pilkington, TEC-15) by the doctor-blade technique and then dried. This doctor-blade procedure was repeated to get a 19 μm thick layer consisting of 14 nm sized anatase TiO_2 nanoparticles. The TiO_2 nanoparticles were synthesized using the continuous supercritical fluid reactor at Department of Chemistry, Aarhus University,[27−29] and detailed preparation procedures and components of the TiO_2 pastes were reported in our previous work.[30] After doctor-blading, the TiO_2 layers were annealed at 550 °C for two hours in air, resulting in mesoporous TiO_2 film electrodes. Then the electrodes were further treated in 40 mM $TiCl_4$ solution, rinsed, dried, and heated to 500 °C

dx.doi.org/10.1021/am302360g | ACS Appl. Mater. Interfaces 2013, 5, 795−800

in a hot air stream for 30 min. After cooling to 80 °C, the electrodes immersed into a 0.3 mM ethanol solution of N719 dye ($RuL_2(SCN)_2{\cdot}2H_2O$, L = 2,2′-bipyridyl-4,4′-dicarboxylic acid, Dyesol) overnight. The dye sensitized TiO_2 electrodes were rinsed with ethanol and dried in the air before usage.

Preparation of Flexible Pt CEs. The process of preparing Pt electrodes on ITO-PET is shown in Figure 1a. Graphite sheets (40 mm × 45 mm × 2 mm, Haimen Shuguang Carbon Industry Co. Ltd.) were first pretreated with emery paper to get a smooth surface that makes Pt particles can be transferred more easily. Then H_2PtCl_6 (30 mM in isopropanol) was screen printed on the smooth surface of the graphite substrates, followed by sintering at 385 °C for 30 min. After cooling down to the room temperature, the Pt particles on the graphite substrates covered with ITO-PET (13Ω/□, Tobi) substrates were pressed under 50 MPa (Pt/ITO-L) and 100 MPa (Pt/ITO-H) for 20 min, respectively. Finally the Pt particles were transferred to the ITO-PET substrates. For comparison, a Pt/FTO electrode fabricated by thermal decomposition at 385 °C on rigid FTO glass was also prepared.[24]

Fabrication of DSCs. The dye-sensitized nanocrystalline TiO_2 electrodes and counter electrodes were assembled by sandwiching the electrolyte solution, which was composed of 0.6 M methylhexy limidazolium iodide, 0.1 M iodine, 0.5 M tert-butylpyridine, and 0.1 M lithium iodide in 3-methoxypropionitrile. The active cell area is 0.15 cm^2.

Characterization. The morphologies of press-transferred Pt particles on ITO-PET substrates were investigated by scanning electron microscopy (SEM, FEIXL30 S-FEG).

Cyclic voltammetries (CVs) was carried out using a Pt wire as auxiliary electrode, an Ag/Ag^+ electrode as reference electrode and the fabricated Pt electrode as working electrode with a total exposure area of 0.5 cm^2. in an acetonitrile solution containing 0.1 M $LiClO_4$, 10 mM LiI, and 1 mM I_2. The scan rate was 100 mV/s and the data were acquired by a CHI 660D electrochemical workstation (CH Instruments).

Electrochemical impedance spectroscopy (EIS) measurements were studied using the IM6ex electrochemical workstation with the frequency range from 100 mHz to 100 kHz. The amplitude of the modulated signal was 10 mV.

Transmittance of the counter electrodes was obtained by a UV−vis spectrophotometer (Shimadzu UV-2550 spectroscope) in the wavelength range of 400−800 nm.

To test the photovoltaic behavior, a solar light simulator (Oriel, 91192) was used to provide an illumination of 100 mW/cm2 (AM 1.5) on the surface of the solar cells. The incident light intensity was calibrated with a radiant power energy meter (Oriel, 70260) before each experiment. The current−voltage curves were recorded by a potentiostat (Princeton Applied Research, model 263A).

3. RESULTS AND DISCUSSION

The appearance and morphology of Pt particles on substrates have great impact on the properties of counter electrodes. Figure 2 shows the surface morphology of the transferred Pt particles on different substrates. As seen in Figure 2a, the bare surface of ITO-PET is quite flat. In images b and c in Figure 2, it can be clearly observed that Pt nanoparticles form well-separated and uniformly distributed Pt clusters on the ITO-PET and graphite sheet, which means that transferring procedure did not change the distribution and morphology of the Pt clusters. However, the number of Pt particles on transferred electrodes is slightly less than that on the graphite sheet, indicating that only particles larger than a certain size can be transferred from graphite sheets to the plastic substrates. Since the surfaces of graphite sheets were still not flat enough, some small clusters of Pt cannot completely contact with the ITO-PET during this procedure. Compared with the Figure 2d, which shows Pt CEs on rigid FTO glass, the transferred Pt on the ITO-PET shows fewer Pt clusters that are also smaller in size.

Before applying the Pt electrodes prepared by different methods, cyclic voltammetries (CVs) was carried out using a three electrode electrochemical system with a scan rate of 100 mV/s. Figure 3 shows the cyclic voltammetries curves of Pt/ITO-L, Pt/ITO-H, and Pt/FTO electrodes. Two pairs of redox peaks were observed in all curves. The relative negative pair is assigned to the redox reaction 1 and the positive is assigned to redox reaction 2

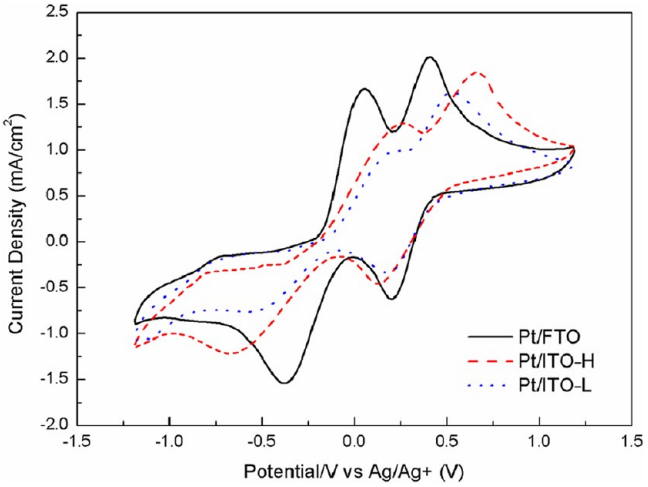

Figure 3. Cyclic voltammograms of the three Pt CEs for the triiodide/iodide redox couple.

$$I_3^- + 2e^- = 3I^- \quad (1)$$

$$2I_3^- = 3I_2 + 2e^- \quad (2)$$

The peak potentials of the three electrodes are similar, which means that the redox reaction was reversible with all the three electrodes. Although both transferred Pt CEs' curves in the figure exhibit lower peak current densities than that of Pt/FTO, it can be concluded that the enhancement of pressure improves the peak values of the transferred electrodes. This means that the transferred electrodes with higher pressure have a better electrochemical activity because of the improved adhesion between the Pt particles and plastic substrate. Pt/ITO-H and Pt/FTO show closed peak current densities, demonstrating that these two electrodes possess a similar electrochemical activity toward the triiodide/iodide redox reaction.

To further assess the catalytic activity of the CEs in triiodide/iodide, the interfacial charge transfer resistance (R_{CT}) was measured by electrochemical impedance spectroscopy (EIS) measurements with typical cells (shown in Figure 4a) receiving an illumination of 100 mW/cm^2 (AM 1.5) on an active area of the device is 0.5 cm^2. The equivalent circuit for this type of cell is shown in Figure 4(b). In the Nyquist plot, the first semicircle is attributed to the impedance of the charge transfer process at the CEs (R_{CT1}) and the second semicircle is related to the charge transfer processes for the TiO_2/dye/electrolyte interface (R_{CT2}). In Figure 4d, it can be observed that the R_{CT2} values are constant for the three electrodes since R_{CT2} is related to TiO_2/dye/electrolyte interface, whereas the R_{CT1} values depended on the properties of Pt CEs and therefore are much different. The R_{CT1} of Pt/ITO-L was 30.3 Ω, which was much higher than that of the other two CEs. Furthermore, as seen in Figure 4c,

dx.doi.org/10.1021/am302360g | ACS Appl. Mater. Interfaces 2013, 5, 795−800

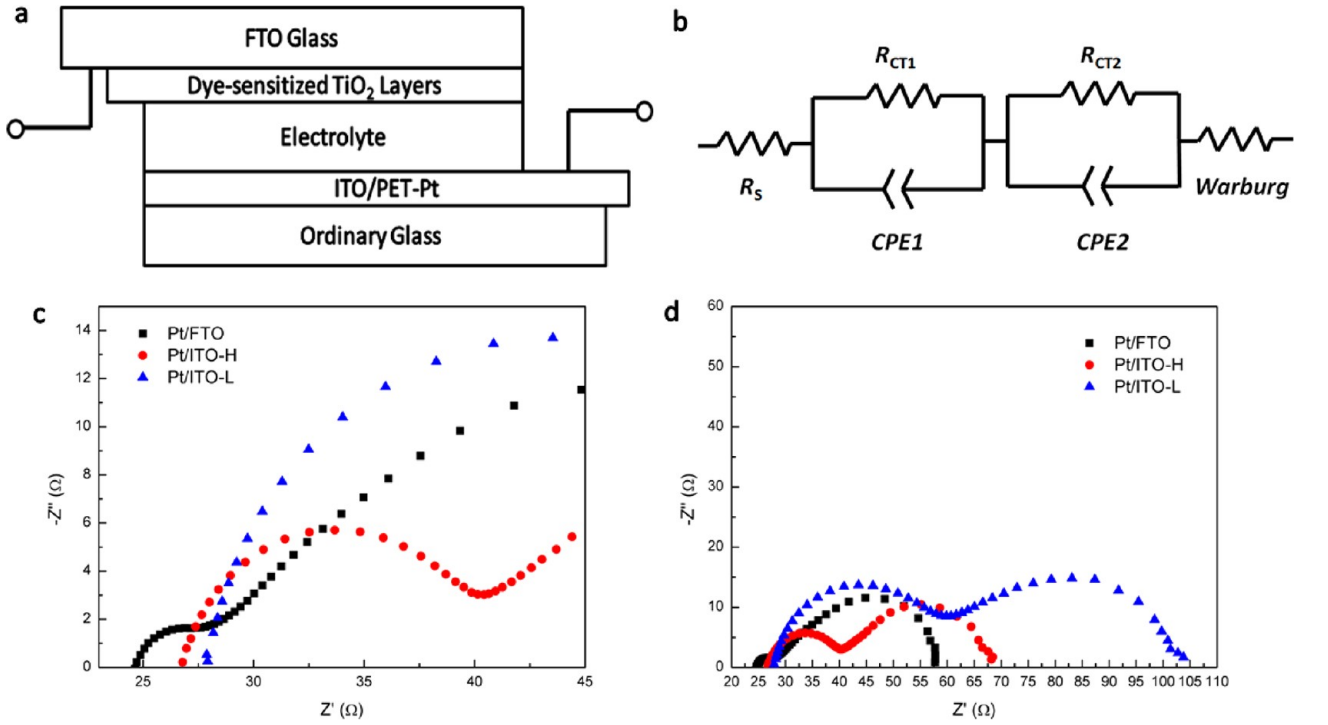

Figure 4. (a) Electrochemical cell used for measurement of the impedance spectrum, (b) equivalent circuit of the typical device. (c) Nyquist plot of the expanded range of the ordinate and abscissa from (d) Nyquist plots of the cells. The active area is 0.5 cm^2.

which shows the expanded range of the ordinate and abscissa from Nyquist plots, R_{CT1} of Pt/ITO-H (13.8 Ω) was relatively low, although still slightly higher than Pt/FTO (3.2 Ω). This results from the fact that press-transferred electrodes have a smaller number of Pt particles and a weaker adhesion with the substrates, as described above.

Since the back-illuminated efficiencies of the devices are directly related to the amount of incident light, it is necessary to study the transparency of the CEs. Figure 5 compares the transparency of transferred Pt/ITO CEs obtained with two different pressures and the traditional thermal deposition electrode. The average transmittances between 400 to 800 nm of the two transferred CEs are 74.5 and 72.5%, respectively, which are both higher than that of Pt/FTO CEs (70.6%). The superior transmittance of the transferred electrodes with lower pressure is expected since a higher pressure results in more Pt particles being transferred from the graphite sheet to ITO/PET substrates. However, even under the largest pressure, the transferred electrodes still have an improved transparency compared with traditional electrodes.

The photocurrent−voltage (I−V) curves of front-side illuminated photovoltaic performance are shown in Figure 6 with Pt/ITO-L CE, Pt/ITO-H CE and Pt/FTO CE under standard simulated AM 1.5 illumination at 100 mW/cm^2. The photovoltaic parameters are listed in Table 1. In front-side illuminated photovoltaic performance, a low FF for transferred CE with low pressure is observed, leading to a relatively poor performance of the device (5.51%) compared with the 7.62%

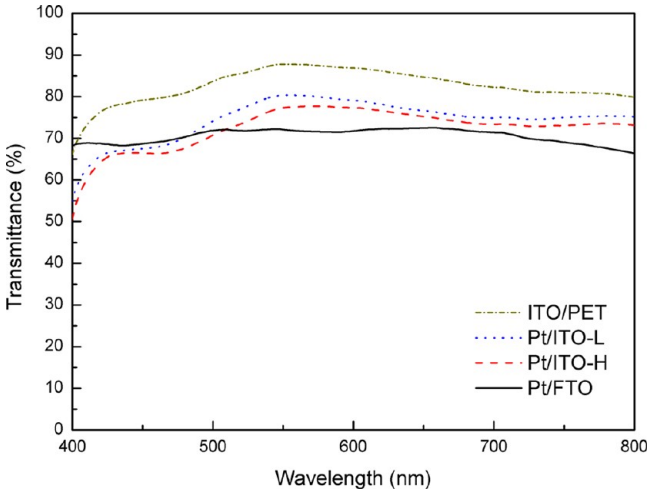

Figure 5. Optical transmittance of the Pt CEs on ITO/PET with different pressures and FTO glass.

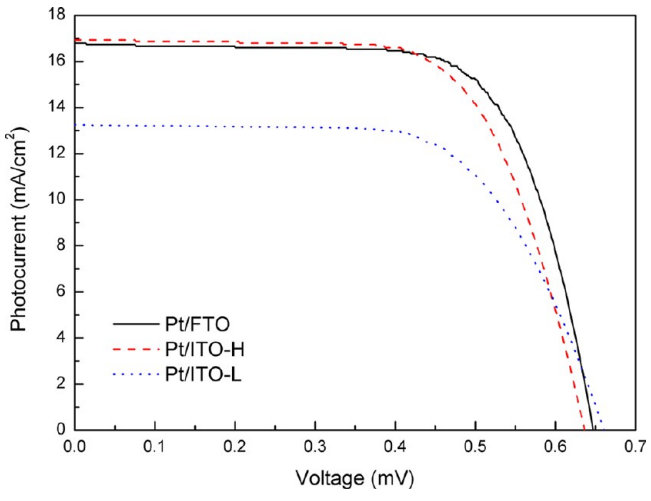

Figure 6. Photocurrent−voltage curves for front-side illuminated DSCs with three Pt counter electrodes.

dx.doi.org/10.1021/am302360g | ACS Appl. Mater. Interfaces 2013, 5, 795−800

Table 1. Photovoltaic Parameters of the Front-Side Illuminated DSCs with Different Pt CEs

illumination side	substrates	J_{sc}(mA/cm^2)	V_{oc}(mV)	FF	η (%)
front	FTO	16.77	647	0.70	7.62
	ITO-H	16.79	636	0.68	7.21
	ITO-L	13.72	658	0.61	5.51

conversion efficiency obtained for the cell using Pt/FTO CE. The FF can be improved from 0.61 to 0.68 by enhancing the pressure during the transfer procedure and this leads to a conversion efficiency of 7.21% for the DSC with Pt/ITO-H CE. Thus, the high-pressure transfer electrode reaches more than 94% efficiency of conventional CEs. In general, the slightly lower FF and J_{SC} of Pt/ITO-H are due to its lower R_{CT1}. The results are in good accordance with the CVs and EIS analysis discussed before.

The photocurrent−voltage curves of the DSCs with back-side illumination are presented in Figure 7. The relative

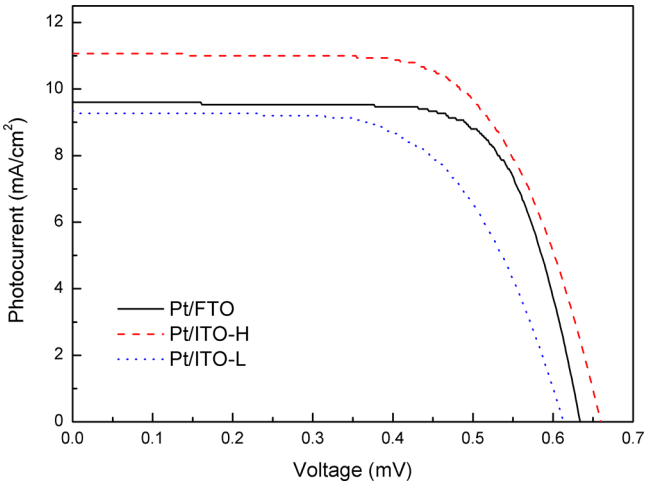

Figure 7. Photocurrent−voltage curves for back-side illuminated DSCs with three Pt counter electrodes.

Table 2. Photovoltaic Parameters of the Back-Side Illuminated DSCs with Different Pt CEs

illumination side	substrates	J_{sc}(mA/cm^2)	V_{oc}(mV)	FF	η (%)
back	FTO	9.71	633	0.70	4.32
	ITO-H	10.99	660	0.67	4.86
	ITO-L	9.25	614	0.63	3.58

parameters are listed in Table 2. Because of the high transmittance through the transferred Pt CEs in visible region, Pt/ITO-H obtains a superior conversion efficiency of 4.86% with a higher J_{SC} of 10.99 mA/cm^2. In the contrast, Pt/FTO only has an efficiency of 4.32% with J_{SC} of 9.71 mA/cm^2. This result can be explained by the optical transmittances that were discussed in the previous section. Pt/FTO CE is much darker and it has a stronger absorption, whereas the transferred CEs let more light reach the inside of the device leading to a higher photocurrent. This means that the press-transfer method is a highly suitable technique for preparation of Pt CEs with high transparency and excellent performance at either front or back side illumination.

4. CONCLUSIONS

We have developed a press-transfer method, which was successfully utilized to prepare Pt CEs on flexible ITO-PET substrates. The morphology, reaction activity, interfacial charge transfer resistance and optical transmittance of the electrodes were examined. The press-transferred Pt CEs exhibited an excellent catalytic activity in I^-/I_3^- electrolyte, and achieved remarkable front- and back-side illuminated efficiencies of 7.21 and 4.86%, respectively. It is believed that the transferred Pt CEs with high transparency are competitive with conventional thermal deposited electrodes. Furthermore, this new method for fabricating flexible transparent Pt CEs has considerable promise because of its low cost, simplicity, and potential application in roll-to-roll techniques.

AUTHOR INFORMATION

Corresponding Authors

*Tel. /Fax: +86-10-8264-9242. E-mail: qbmeng@iphy.ac.cn.
*Tel. /Fax: ++45 − 8715- 5982. Email: bo@chem.au.dk.

Notes

The authors declare no competing financial interest.

ACKNOWLEDGMENTS

The authors appreciate the financial supports of National Key Basic Research Program (973 project, 2012CB932903), National Natural Science Foundation of China (20725311, 51072221 and 21173260) and the Knowledge Innovation Program of the Chinese Academy of Sciences (KJCX2-YW-W27).

REFERENCES

(1) Peter, L. M. *J. Phys. Chem. Lett.* **2011**, *2*, 1861.
(2) Yella, A.; Lee, H. W.; Tsao, H. N.; Yi, C.; Chandiran, A. K.; Nazeeruddin, M. K.; Diau, E. W. G.; Yeh, C. Y.; Zakeeruddin, S. M.; Grätzel, M. *Science* **2011**, *334*, 629.
(3) Park, J. H.; Jun, Y.; Yun, H.; Lee, S.; Kang, M. G. *Electrochem. Soc.* **2008**, *155* (7), F145−9.
(4) Yamaguchi, T.; Tobe, N.; Matsumoto, D.; Nagai, T.; Arakawa, H. *Sol. Energy. Mater. Sol. Cells* **2010**, *94* (5), 812−6.
(5) Ito, S.; Ha, N. C.; Rothenberger, G.; Liska, P.; Comte, P.; Zakeeruddin, S. M. *Chem. Commun.* **2006**, *38*, 4004−6.
(6) Wu, M. X.; Lin, X.; Hagfeldt, A.; Ma, T. L. *Angew. Chem.* **2011**, *123*, 3582.
(7) Lin, X.; Wu, M. X.; Wang, Y. D.; Hagfeldt, A.; Ma, T. L. *Chem. Commun.* **2011**, *47*, 11489−11491.
(8) Sun, H,C.; Qin, D.; Huang, S. Q.; Guo, X. Z.; Li, D. M.; Luo, Y. H.; Meng, Q. B. *Energy. Environ. Sci.* **2011**, *4*, 2630.
(9) Lee, K. M.; Hsu, C. Y.; Chen, P. Y.; Ikegami, M.; Miyasaka, T.; Ho, K. C. *Phys. Chem. Chem. Phys.* **2009**, *11*, 3375−3379.
(10) Sun, H. C.; Luo, Y. H.; Meng, Q. B. *J.Phys. Chem. C* **2010**, *114* (26), 11673−11679.
(11) Tai, Q.; Chen, B.; Guo, F.; Xu, S.; Hu, H.; Sebo, B.; Zhao, X. Z. *ACS Nano* **2011**, *5*, 3795−3799.
(12) Huang, Z.; Liu, X. H.; Li, K. X.; Li, D. M.; Luo, Y. H.; Li, H.; Song, W. B.; Chen, L. Q.; Meng, Q. B. *Electrochem. Commun.* **2007**, *9* (4), 596−598.
(13) Li, K. X.; Luo, Y. H.; Yu, Z. X.; Deng, M. H.; Li, D. M.; Meng, Q. B. *Electrochem. Commun.* **2009**, *11* (7), 1346−1349.
(14) Chen, J.; Li, K.; Luo, Y.; Guo, X.; Li, D.; Deng, M. *Carbon* **2009**, *47* (11), 2704−8.
(15) Fang, X. M.; Ma, T. L.; Guan, G. Q.; Akiyama, M.; Kida, T.; Abe, E. *J. Electroanal. Chem.* **2004**, *570*, 257−263.
(16) Ma, T. L.; Fang, X. M.; Akiyama, M.; Inoue, K.; Noma, H.; Abe, E. *J. Electroanal. Chem.* **2004**, *574*, 77−83.

(17) Fang, X.; Ma, T.; Akiyama, M.; Guan, G.; Tsunematsu, S.; Abe, E. *Thin Solid Films* **2005**, *472* (1−2), 242−5.
(18) Kang, M. G.; Park, N.; Ryu, K. S.; Chang, S. H.; Kim, K. *Sol. Energy. Mater. Sol. Cells* **2006**, *903*, 574−81.
(19) Jun, Y.; Kim, J.; Kang, M. G. *Sol. Energy. Mater. Sol. Cells* **2007**, *91* (9), 779−84.
(20) Chen, L. L.; Tan, W. W.; Zhang, J. B.; Zhou, X. W.; Zhang, X. L.; Lin, Y. *Electrochim. Acta* **2010**, *55*, 3721−3726.
(21) Nemoto, J.; Sakata, M.; Hoshi, T.; Ueno, H.; Kaneko, M. *J. Electroanal. Chem.* **2007**, *599* (1), 23−30.
(22) Fu, N. Q.; Xiao, X. T.; Zhou, X. W.; Zhang, J. B.; Lin, Y. *J. Phys. Chem. C* **2012**, *116*, 2850−2857.
(23) Chen, L.; Tan, W.; Zhang, J.; Zhou, X.; Zhang, X.; Lin, Y. *Electrochim. Acta* **2010**, *55* (11), 3721−6.
(24) Papageorgiou, N.; Maier, W. F.; Gratzel, M. *J. Electrochem. Soc.* **1997**, *144* (3), 876−884.
(25) Huang, X. M.; Yu, Z. X.; Huang, S. Q.; Zhang, Q. X.; Li, D. M.; Luo, Y. H.; Meng, Q. B. *Mater. Lett.* **2010**, *64* (15), 1701−1703.
(26) Huang, X. M.; Huang, S. Q.; Zhang, Q. X.; Guo, X. Z.; Li, D. M.; Luo, Y. H.; Shen, Q.; Toyoda, T.; Meng, Q. B. *Chem. Commun.* **2011**, *47* (9), 2664−2666.
(27) Becker, J.; Hald, P.; Bremholm, M.; Pedersen, J. S.; Chevallier, J.; Iversen, S. B.; Iversen, B. B. *ACS Nano* **2008**, *2*, 1058−1068.
(28) Hald, P.; Becker, J.; Bremholm, M.; Pedersen, J. S.; Chevallier, J.; Iversen, S. B.; Iversen, B. B. J. *Solid State Chem.* **2006**, *179*, 2674−2680.
(29) Toft, L. L.; Aarup, D. F.; Bremholm, M.; Hald, P.; Iversen, B. B. J. *Solid State Chem.* **2009**, *182*, 491−495.
(30) Li, C. H.; Luo, Y. H.; Guo, X. Z.; Li, D. M.; Mi, J. L.; Lasse, S.; Hald, Peter.; Meng, Q. B.; Iversen, B. B. *J. Solid State Chem.* **2012**, *196*, 504−510.